

Intermediate-depth earthquakes facilitated by eclogitization-related stresses

Junichi Nakajima^{1*}, Naoki Uchida¹, Takahiro Shiina¹, Akira Hasegawa¹, Bradley R. Hacker², and Stephen H. Kirby³

¹Research Center for Prediction of Earthquakes and Volcanic Eruptions, Graduate School of Science, Tohoku University, Sendai 980-8578, Japan

²Earth Research Institute, University of California–Santa Barbara, Santa Barbara, California 93106-9630, USA

³U.S. Geological Survey, Menlo Park, California 94025, USA

ABSTRACT

Eclogitization of the basaltic and gabbroic layer in the oceanic crust involves a volume reduction of 10%–15%. One consequence of the negative volume change is the formation of a paired stress field as a result of strain compatibility across the reaction front. Here we use waveform analysis of a tiny seismic cluster in the lower crust of the downgoing Pacific plate and reveal new evidence in favor of this mechanism: tensional earthquakes lying 1 km above compressional earthquakes, and earthquakes with highly similar waveforms lying on well-defined planes with complementary rupture areas. The tensional stress is interpreted to be caused by the dimensional mismatch between crust transformed to eclogite and underlying untransformed crust, and the earthquakes are probably facilitated by reactivation of fossil faults extant in the subducting plate. These observations provide seismic evidence for the role of volume change–related stresses and, possibly, fluid-related embrittlement as viable processes for nucleating earthquakes in downgoing oceanic lithosphere.

INTRODUCTION

Generation of intermediate-depth earthquakes is an ongoing enigma because high lithostatic pressures render ordinary dry frictional failure unlikely. Earthquakes in subducting oceanic crust have been linked to the transformation of basalt to eclogite and concomitant dehydration (e.g., Kirby et al., 1996; Preston et al., 2003; Hacker et al., 2003). A major, untested prediction of this hypothesis is, however, that the large (10%–15%) volume reduction during eclogite formation should produce a paired stress regime along the eclogitization reaction front in which tension is underlain by compression (Hacker, 1996; Kirby et al., 1996). This study presents the first seismological evidence of such a paired stress field associated with eclogite formation in the oceanic crust.

DATA ANALYSIS

The Pacific plate beneath northeastern Japan has a well-developed double seismic zone in which earthquakes with downdip compression dominate the upper seismic zone within the crust, and earthquakes with downdip tension dominate the lower seismic zone 30–40 km deeper within the mantle (e.g., Hasegawa et al., 1978). Somewhat-isolated seismic clusters are observed locally in the upper seismic zone at a depth of ~150 km (red and pink arrows in Fig. 1A). We investigate seismic features of the most-active isolated seismic cluster (red arrow) using high-quality waveform data. Hypocenters of the cluster relocated by the double-difference method (hypoDD) (Waldhauser and Ellsworth, 2000) with catalog-derived differential data

show that the cluster is located in the lowermost part of the oceanic crust (Fig. 1B) and concentrated in a volume no more than 2 km × 2 km × 5 km (Figs. 1C and 1D). The earthquakes in the cluster have occurred not in swarms but fairly evenly over time (Fig. 1E).

We selected 106 earthquakes ($M \geq 2$) in the period from January 2003 to February 2011, and classified the earthquakes into subgroups on the basis of waveform similarity. A time window of 30 s was set for the vertical component, beginning 3 s before the onset of the P wave, and coherency was calculated using the cross spectral method (Poupinet et al., 1984) for each pair of earthquakes in a frequency band of 2–12 Hz. When the calculated coherencies were larger than 0.9 at three or more stations, we regarded the earthquake pair as part of the same group. In this manner, we categorized 30 earthquakes into nine groups with similar waveforms (Fig. 1F; Fig. DR1 in the GSA Data Repository¹): four groups (R1–R4) of 19 reverse-fault earthquakes and five groups (N1–N5) of 11 normal-fault earthquakes.

For precise relative earthquake relocations, traveltime differences of the 30 earthquakes were calculated using the cross spectral method for both P and S waves. A time window of 3 s was set 0.5 s before the onset of each wave, and delay times were calculated from the phases of cross spectra in a frequency band of 2–12 Hz with a coherency of >0.8 . To avoid half-cycle

skipping of waveforms due to polarity reversal, we calculated traveltime differences independently for the reverse- and normal-fault groups. We applied hypoDD to the calculated differential traveltime data, and determined the relative locations of the earthquakes in the reverse- and normal-fault groups with the one-dimensional velocity model (Ueno et al., 2002).

The relative locations of the reverse-fault earthquakes with respect to the normal-fault earthquakes were determined using S–P time differences. The polarity of waveform was reversed for the normal-fault earthquakes, and their coherencies with the reverse-fault earthquakes were calculated in the same manner as for the earthquake classification. Then, we identified the earthquake pair with the most-similar waveform (an average coherency of 0.92) (Fig. DR2). For this pair, we calculated S–P time differences at 14 common stations based on waveform similarity, and determined the relative locations of the two earthquakes using the S–P time differences. Finally, we shifted the other earthquakes with respect to that earthquake pair.

To estimate the extent of source areas, we determined the source radii of the 30 earthquakes from corner frequencies. Corner frequencies were estimated by applying the spectral ratio method to P-wave amplitude spectra for a tapered 2.0 s time window of the vertical component (e.g., Frankel and Wennerberg, 1989) (Fig. DR3). We used an omega-square source model (Brune, 1970) to model the spectral ratio stacked for the available station pairs. As a result, we obtained the corner frequencies of eight earthquakes. The source radii of the eight earthquakes were calculated using the circular crack model (Sato and Hirasawa, 1973). For the 22 earthquakes without the estimates of corner frequencies, we calculated the source radii from the average stress drop (7 MPa) using the formula of Eshelby (1975). The radii of source areas thus calculated range from 43 m to 216 m with stress drops of 3.5–33.3 MPa. Source parameters obtained for the 30 earthquakes are listed in Table DR1 in the Data Repository.

RESULTS AND DISCUSSION

The relocated hypocenters show important features in terms of earthquake-generating stress and seismic rupture areas. (1) The normal-fault

¹GSA Data Repository item 2013179, Figures DR1–DR3, and Table DR1, is available online at www.geosociety.org/pubs/ft2013.htm, or on request from editing@geosociety.org or Documents Secretary, GSA, P.O. Box 9140, Boulder, CO 80301, USA.

*E-mail: nakajima@aob.gp.tohoku.ac.jp.

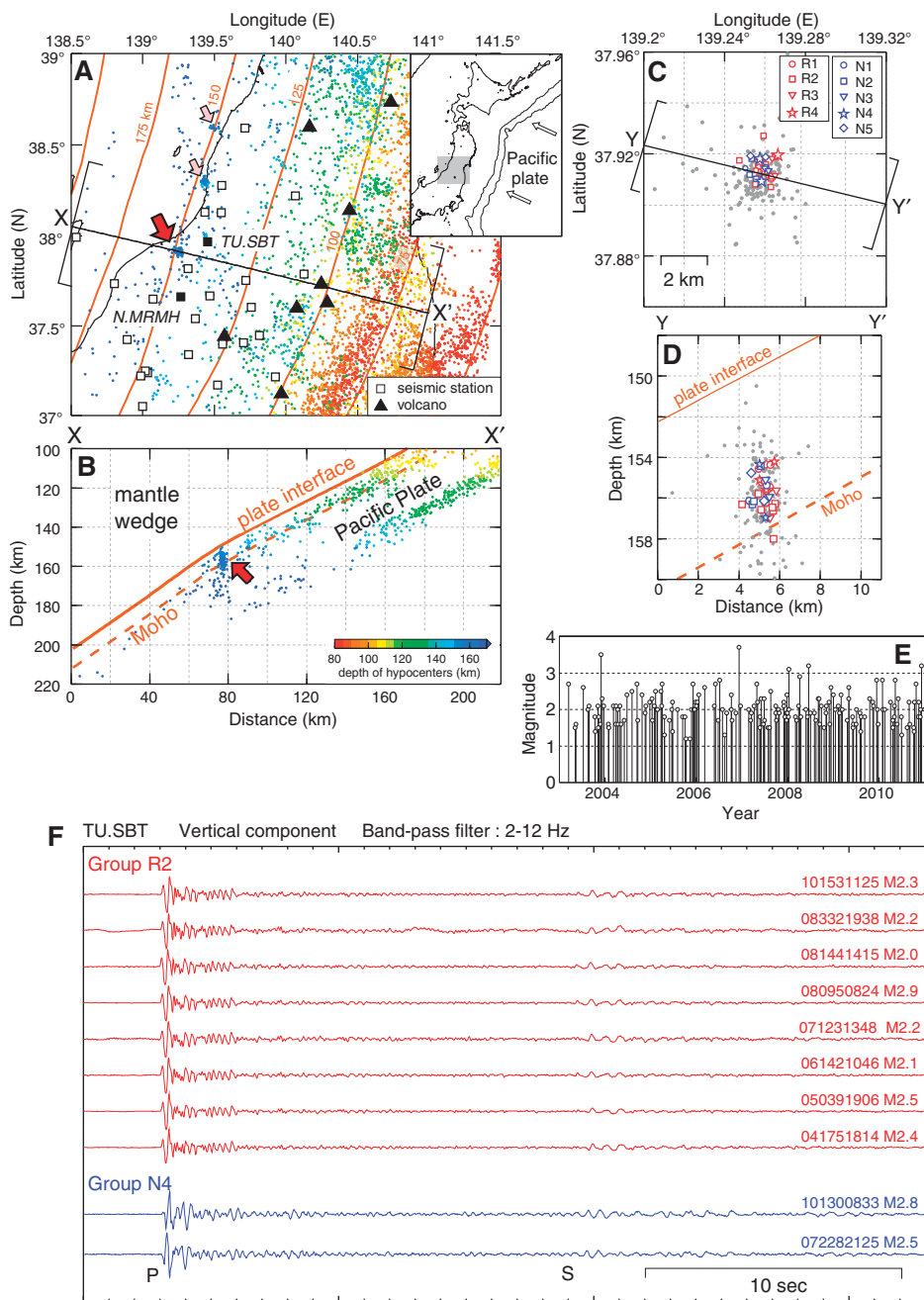


Figure 1. A: Map of earthquakes with focal depths >80 km (colored circles). Orange lines denote the geometry of the Pacific plate (Zhao et al., 1997). Red arrow indicates the seismic cluster analyzed in this study, and pink arrows indicate other isolated clusters. B: Vertical cross section along line X–X' in A. C: Close-up map of the seismic cluster indicated by a red arrow in A. Red and blue symbols are 19 reverse-fault and 11 normal-fault earthquakes, respectively, relocated using catalog-derived differential traveltime data. Earthquakes not analyzed in this study shown in gray. D: Vertical cross section along line Y–Y' in C. E: Magnitude versus time for earthquakes in the seismic cluster. F: Examples of waveforms for earthquakes classified as groups R2 (red) and N4 (blue) recorded at station TU.SBT.

earthquakes lie above the reverse-fault earthquakes, and the distance between the two types is only ~1 km (Fig. 2). (2) All the earthquakes in each subgroup are concentrated in a volume with dimensions of hundreds of meters and define a plane that is consistent with one of the nodal planes of the focal mechanisms. (3) Seven of the nine groups have fault planes that

strike within 30° of the subducting Pacific plate (Fig. 2). (4) Even though some rupture areas may overlap, the earthquakes in the same subgroup appear to have ruptured the fault plane complementarily (Fig. 3; Fig. DR1).

As downdip compression is dominant in the upper seismic plane beneath northeastern Japan (e.g., Hasegawa et al., 1978; Igarashi et al.,

2001), some special process must produce local tension. What process can generate earthquakes with local tension in proximity to compressional earthquakes and produce clusters of seismic events on well-defined and separate planes?

Progressive eclogitization of the oceanic crust of subducting slabs is interpreted from gradual increases in seismic velocities and the disappearance of seismic activity (e.g., Helffrich, 1996; Abers, 2005; Kita et al., 2006). The upper, basaltic layer of the crust transforms to eclogite more easily because of finer grain size, increased alteration, and higher temperatures (e.g., Hacker, 1996); eclogitization of basalt beneath northeastern Japan is interpreted to occur at depths of 70–130 km (Igarashi et al., 2001; Kita et al., 2006). Transformation of the lower, gabbroic layer to eclogite is, however, retarded because of coarser grain size, substantially less alteration, and lower temperatures (e.g., Hacker, 1996); because of this, eclogitization likely progresses from the top of the crust downward (Fig. 4). A low-velocity layer at the top of the Pacific slab suggests that eclogitization of the gabbroic layer is incomplete even at depths down to 150 km (Matsuzawa et al., 1986) where the seismic cluster described here is located.

One possibility to explain the observed seismic cluster is that the eclogitic and gabbroic layers in the slab have different strengths and respond differently to the slab stress state. This is almost certainly true, but whether eclogite is stronger or weaker than gabbro at the conditions of interest is unclear: eclogite is expected to be stronger than gabbro for a given grain size and H₂O content because of the presence of garnet (Wang et al., 2012), but strain localization or fluid can invert this relationship (Austheim, 1991). The prevalence of downdip compressional events in the upper seismic plane suggests that the stronger layer is under compression. Because the seismic cluster described here is composed of tensional events overlying compressional events, the gabbroic layer is carrying the load and the eclogitic layer is weaker.

A second possibility involves transformation-induced stress. Because the transformation of gabbro to eclogite involves a volume reduction of 10%–15% (e.g., Hacker et al., 2003), tension is expected in the transformed (densified) crust and compression is expected in the underlying untransformed crust, as a consequence of a dimensional mismatch between the transformed and untransformed crust (Hacker, 1996). The tension thus generated would be larger than the compression produced by slab unbending (Kirby et al., 1996; Wang, 2002), thereby promoting normal faulting in the transformed crust.

Metamorphism of the igneous oceanic crust to eclogite is an inescapable result of the subduction process, and the negative volume change associated with eclogite-forming reactions is

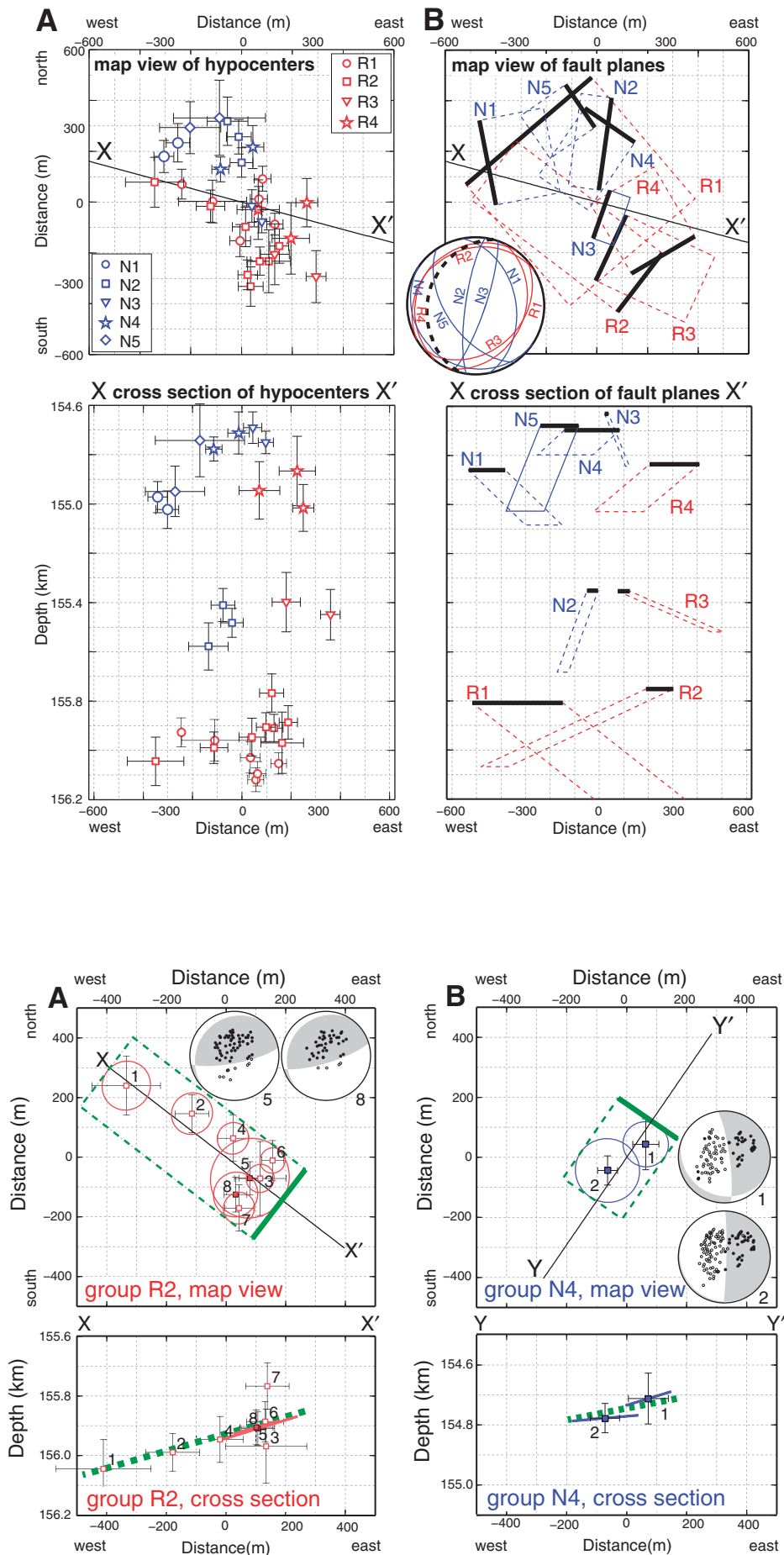


Figure 2. A: Hypocenters relocated by waveform-derived differential data in map view (top) and cross-sectional view (bottom) along line X–X'. Red and blue symbols denote 19 reverse-fault and 11 normal-fault earthquakes, respectively, and bars represent location errors. **B:** Distribution of fault planes for each subgroup in map view (top) and cross-sectional view (bottom). Fault plane is determined from focal mechanism solutions, and its extent is estimated from source areas. A thick line on a rectangle represents the updip end of each fault. Equal-area, lower-hemisphere projections show the fault plane for each subgroup (colored lines) and the strike and dip of the plate interface (black dashed line).

among the largest in rocks (e.g., Hacker et al., 2003). We propose that local eclogitization-related stresses preferentially facilitate reactivation of fossil faults that formed at the trench–outer slope, resulting in the seismic cluster with tension underlain by compression across the eclogitization reaction front. H₂O released by eclogitization may contribute to brittle failure by weakening the faults. The abrupt changes in focal mechanisms reported in this study are the most straightforward evidence yet of the expected stress fields associated with mineralogical changes in the downgoing oceanic plate (Fig. 4). In actual fact, differences in grain size and degree of hydrothermal alteration in the crust will result in lateral variations in eclogitization during subduction (Hacker, 1996). Such lateral variations in eclogitization will yield a local fluctuation of the reaction front, causing three-dimensional variations in the positions of tensional and compressional earthquakes such as groups R3, R4, and N2.

Normal-fault earthquakes interpreted to be associated with eclogite formation are widespread just beneath the slab surface at depths of 70–130 km (Igarashi et al., 2001; Kita et al., 2006). The elevated seismicity at these depths may conceal isolated seismic clusters of the type that we observed at a depth of ~150 km.

Figure 3. Fault planes and source areas for group R2 (A) and group N4 (B). The series of events in each subgroup is numbered in order of occurrence. Colored squares denote earthquakes for which we have determined focal mechanisms. Focal mechanisms are shown in equal-area, lower-hemisphere projections; solid and open circles indicate compressional and dilatational first motions, respectively. Green rectangle represents an apparent fault plane. Cross-sectional views show hypocenters along lines X–X' and Y–Y' in upper panel. Colored lines denote the dip of one nodal plane of focal mechanism solutions. Dashed green line marks the average dip of the fault plane calculated from focal mechanism solutions.

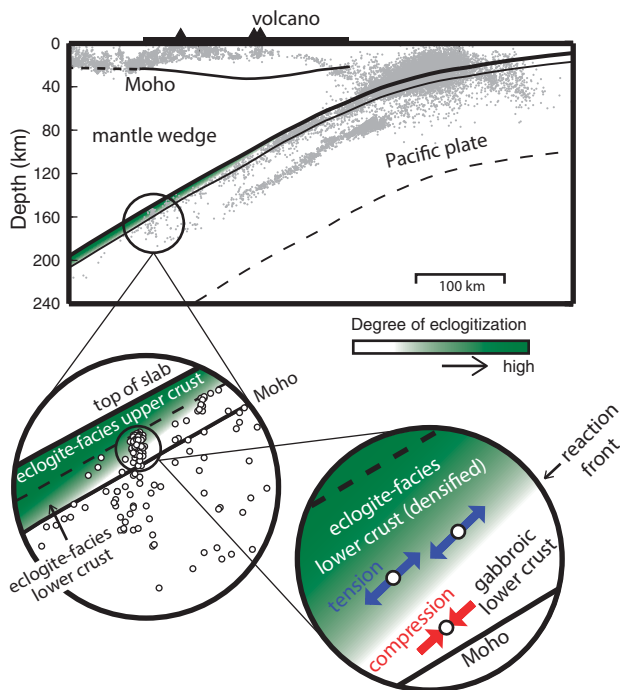


Figure 4. Schematic cartoon of abrupt changes in stress regime along the reaction front where subducting igneous crust transforms to eclogite.

Perhaps the concentrated stress and deformation states that result from eclogitization are visible only where the upper-plane seismicity is waning at depths beyond 150 km (e.g., red and pink arrows in Fig. 1A). If so, seismic clusters of the type that we focused on should become visible under further scrutiny.

ACKNOWLEDGMENTS

We thank T. Matsuzawa for comments and discussions. Constructive reviews by two anonymous reviewers and Editor S.J. Wyld improved the manuscript. We used arrival-time data in the unified catalog by the Japan Meteorological Agency, and waveform data observed at a nationwide seismograph network. This work was supported by the Ministry of Education, Culture, Sports, Science and Technology of Japan, under its Observation and Research Program for Prediction of Earthquakes and Volcanic Eruptions; by the Global COE Program, Global Education and Research Center for Earth and Planetary Dynamics, Tohoku University; and by U.S. National Science Foundation grant EAR-0745588.

REFERENCES CITED

Abers, G., 2005, Seismic low-velocity layer at the top of subducting slabs: Observations, predictions, and systematics: *Physics of the Earth and Planetary Interiors*, v. 149, p. 7–29, doi:10.1016/j.pepi.2004.10.002.

Austrheim, H., 1991, Eclogite formation and dynamics of crustal roots under continental collision zones: *Terra Nova*, v. 3, p. 492–499, doi:10.1111/j.1365-3121.1991.tb00184.x.

Brune, J.N., 1970, Tectonic stress and spectra of seismic shear waves from earthquakes: *Journal of*

Geophysical Research, v. 75, p. 4997–5009, doi:10.1029/JB075i026p04997.

Eshelby, J.D., 1975, The determination of the elastic field of an ellipsoidal inclusion and related problems: *Proceedings of the Royal Society of London, ser. A*, v. 241, p. 376–396.

Frankel, A., and Wennerberg, L., 1989, Microearthquake spectra from the Anza, California, seismic network: Site response and source scaling: *Bulletin of the Seismological Society of America*, v. 79, p. 581–609.

Hacker, B.R., 1996, Eclogite formation and the rheology, buoyancy, seismicity, and H₂O content of oceanic crust, in Bebout, G.E., et al., eds., *Subduction: Top to bottom: American Geophysical Union Geophysical Monograph* 96, p. 337–346.

Hacker, B.R., Peacock, S.M., Abers, G.A., and Holloway, S.D., 2003, Subduction factory 2. Are intermediate-depth earthquakes in subducting slabs linked to metamorphic dehydration reactions?: *Journal of Geophysical Research*, v. 108, 2030, doi:10.1029/2001JB001129.

Hasegawa, A., Umino, N., and Takagi, A., 1978, Double-planned structure of the deep seismic zone in the northeastern Japan arc: *Tectonophysics*, v. 47, p. 43–58, doi:10.1016/0040-1951(78)90150-6.

Helfrich, G., 1996, Subducted lithospheric slab velocity structure: Observations and mineralogical inferences, in Bebout, G.E., et al., eds., *Subduction: Top to bottom: American Geophysical Union Geophysical Monograph* 96, p. 215–222.

Igarashi, T., Matsuzawa, T., Umino, N., and Hasegawa, A., 2001, Spatial distribution of focal mechanisms for interplate and intraplate earthquakes associated with the subducting Pacific plate beneath the northeastern Japan arc: A triple-planed deep seismic zone: *Journal of Geophysical*

Research, v. 106, p. 2177–2191, doi:10.1029/2000JB900386.

Kirby, S., Engdahl, E.R., and Denlinger, R., 1996, Intermediate-depth intraslab earthquakes and arc volcanism as physical expressions of crustal and uppermost mantle metamorphism in subducting slabs, in Bebout, G.E., et al., eds., *Subduction: Top to bottom: American Geophysical Union Geophysical Monograph* 96, p. 195–214.

Kita, S., Okada, T., Nakajima, J., Matsuzawa, T., and Hasegawa, A., 2006, Existence of a seismic belt in the upper plane of the double seismic zone extending in the along-arc direction at depths of 70–100 km beneath NE Japan: *Geophysical Research Letters*, v. 33, L24310, doi:10.1029/2006GL028239.

Matsuzawa, T., Umino, N., Hasegawa, A., and Takagi, A., 1986, Upper mantle velocity structure estimated from PS-converted wave beneath the northeastern Japan arc: *Geophysical Journal of the Royal Astronomical Society*, v. 86, p. 767–787, doi:10.1111/j.1365-246X.1986.tb00659.x.

Poupinet, G., Ellsworth, W.L., and Frechet, J., 1984, Monitoring velocity variations in the crust using earthquake doublets: An application to the Calaveras Fault, California: *Journal of Geophysical Research*, v. 89, p. 5719–5731, doi:10.1029/JB089iB07p05719.

Preston, A.L., Creager, K.C., Crosson, R.S., Brocher, T.M., and Trehu, A.M., 2003, Intraslab earthquakes: Dehydration of the Cascadia slab: *Science*, v. 302, p. 1197–1200, doi:10.1126/science.1090751.

Sato, T., and Hirasawa, T., 1973, Body wave spectra from propagating shear cracks: *Journal of Physics of the Earth*, v. 21, p. 415–431, doi:10.4294/jpe.1952.21.415.

Ueno, H., Hatakeyama, S., Aketagawa, T., Funasaki, J., and Hamada, N., 2002, Improvement of hypocenter determination procedures in the Japan Meteorological Agency: *Quarterly Journal of Seismology*, v. 65, p. 123–134.

Waldhauser, F., and Ellsworth, W.L., 2000, A double-difference earthquake location algorithm: Method and application to the Northern Hayward fault, California: *Bulletin of the Seismological Society of America*, v. 90, p. 1353–1368, doi:10.1785/0120000006.

Wang, K., 2002, Unbending combined with dehydration embrittlement as a cause for double and triple seismic zones: *Geophysical Research Letters*, v. 29, 1889, doi:10.1029/2002GL015441.

Wang, Y.F., Zhang, J.F., Jin, Z.M., and Green, H.W., 2012, Mafic granulite rheology: Implications for a weak continental lower crust: *Earth and Planetary Science Letters*, v. 353–354, p. 99–107, doi:10.1016/j.epsl.2012.08.004.

Zhao, D., Matsuzawa, T., and Hasegawa, A., 1997, Morphology of the subducting slab boundary in the northeastern Japan arc: *Physics of the Earth and Planetary Interiors*, v. 102, p. 89–104, doi:10.1016/S0031-9201(96)03258-X.

Manuscript received 27 June 2012
Revised manuscript received 18 December 2012
Manuscript accepted 13 January 2013

Printed in USA